

Effect of modulating field on photoreflectance simulated by electroreflectance

S. J. Chiou, Y. G. Sung, D. P. Wang, K. F. Huang, T. C. Huang, and A. K. Chu

Citation: [Journal of Applied Physics](#) **85**, 3770 (1999); doi: 10.1063/1.369746

View online: <http://dx.doi.org/10.1063/1.369746>

View Table of Contents: <http://scitation.aip.org/content/aip/journal/jap/85/7?ver=pdfcov>

Published by the [AIP Publishing](#)

Articles you may be interested in

[Photoreflectance and contactless electroreflectance measurements of semiconductor structures by using bright and dark configurations](#)

Rev. Sci. Instrum. **80**, 096103 (2009); 10.1063/1.3213613

[Interference effects in electromodulation spectroscopy applied to GaAs-based structures: A comparison of photoreflectance and contactless electroreflectance](#)

Appl. Phys. Lett. **86**, 091115 (2005); 10.1063/1.1873052

[Evaluation of modulating field of photoreflectance of surface-intrinsic- n + type doped GaAs by using photoinduced voltage](#)

J. Appl. Phys. **91**, 4101 (2002); 10.1063/1.1453492

[Determination of built-in field by applying fast Fourier transform to the photoreflectance of surface-intrinsic n + - type doped GaAs](#)

Appl. Phys. Lett. **74**, 475 (1999); 10.1063/1.123040

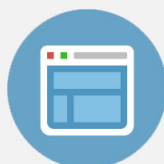
[Micro-electroreflectance and photoreflectance characterization of the bias dependence of the quantum confined Stark effect in a fabricated 0.98 \$\mu\text{m}\$ InGaAs/GaAs/InGaP laser](#)

Appl. Phys. Lett. **70**, 2562 (1997); 10.1063/1.118919



Re-register for Table of Content Alerts

Create a profile.



Sign up today!



Effect of modulating field on photoreflectance simulated by electroreflectance

S. J. Chiou, Y. G. Sung, and D. P. Wang^{a)}

Department of Physics, National Sun Yat-Sen University, Kaohsiung, 80424, Taiwan, Republic of China

K. F. Huang and T. C. Huang

Department of Electro-Physics, National Chiao-Tung University, Hsinchu, Taiwan, Republic of China

A. K. Chu

Department of Electro-optics, National Sun Yat-Sen University, Kaohsiung, Taiwan, Republic of China

(Received 29 October 1998; accepted for publication 10 December 1998)

Photoreflectance (PR) of surface-intrinsic- n^+ (s-i- n^+) type doped GaAs has been simulated by electroreflectance (ER). The simulated spectra of the s-i- n^+ sample have exhibited many Franz-Keldysh oscillations, which enable the electric field (F) to be determined. It is known that F 's determined from PR are subjected to photovoltaic effect and the measured F is close to $F_{\text{bi}} - \delta F/2$ when the modulating field, $\delta F \ll F_{\text{bi}}$, where F_{bi} is the built-in field of the sample and δF is the modulating field. In this work, we have investigated the relation between the measured F and δF not only for the region where $\delta F \ll F_{\text{bi}}$ holds, but also for a whole range of δF . In order to determine the magnitude of δF , we have used ER to simulate PR, that is, the measurements of ER under a forward bias, which is set to be equal to $\delta F/2$. © 1999 American Institute of Physics. [S0021-8979(99)01906-4]

I. INTRODUCTION

Modulation spectroscopy¹⁻⁵ is an important technique for the study and characterization of semiconductor properties. It can yield sharp structures around the critical points and is sensitive to the surface or interface electric fields. Among them, electroreflectance (ER) is used to modulate the electric field strength of samples and photoreflectance (PR) is thought of as a form of contactless ER.

For a medium field strength, the PR or ER spectra exhibit Franz-Keldysh oscillations (FKOs) above the band gap energy. The electric field strength (F) in the depletion region can be deduced from the periods of FKOs.⁶ It is known that the PR or ER of surface-intrinsic- n^+ type doped (s-i- n^+) GaAs exhibit many FKOs and they were attributed to the existence of a uniform electric field in the undoped layer.⁷⁻¹¹ The slow decay of FKOs with energy will allow the more accurate determination of F by using fast Fourier transform technique.^{12,13}

Although PR has the advantage of being contactless, it cannot exclude the photovoltaic effect from the pump and probe beams,^{7,14} especially from the pump beam for its higher intensity. The photovoltage, which was produced by electron-hole pairs generated by the pump and probe beams, will oppose the original built-in voltage. Hence the F in the depletion region is reduced and almost equal to $F_{\text{bi}} - \delta F/2$ when $\delta F \ll F_{\text{bi}}$,¹⁵ where F_{bi} is the built-in field of the sample and δF is the strength of the modulating field. Therefore, in order to reduce the photovoltaic effect, the power densities of the pump (P_{pu}) and probe beams were kept below $10 \mu\text{W}/\text{cm}^2$ in the previous measurements.¹⁶

Recently, we have used fast Fourier transform (FFT) technique to study the dependence of F and FFT line shape on P_{pu} .¹⁷ However, it is difficulty to estimate δF in the PR measurements. In order to know precisely the magnitude of δF , we have simulated PR by ER, that is, by applying the sample at a sum of a modulating square wave with amplitude V_{ac} and a forward bias with the amplitude of $V_{\text{ac}}/2$.

II. EXPERIMENT

The s-i- n^+ GaAs sample used in this experiment was grown on a n^+ -type GaAs(100) substrate by molecular beam epitaxy (MBE). A $1.0 \mu\text{m}$ n^+ -doped GaAs buffer layer was first grown on this substrate, followed by a 1200 \AA undoped GaAs cap layer. The gold film was deposited by a hot filament evaporation and the thickness estimated to be about 70 \AA .

The experimental setup for the PR measurements, which is similar to that previously described in the literature,⁵ will be described briefly. Light from a 200 W tungsten lamp was passed through a 500 mm monochromator (Acton spectra Pro-500). The exit light was defocused onto the sample by a lens. The reflected light was collected by a lens to focus onto a Si photodiode detector. The sample was modulated at 400 Hz by a combination of a square wave and a forward bias with an amplitude of half that of the square wave. The photodiode signal was composed of a dc component (R) and an ac component (ΔR). The dc component (R) was measured by an analog to digital converter card of an IBM compatible personal computer. The output of the photodiode was also fed into a lock-in amplifier (Stanford Research System SR 830) to measure the modulated ac signal (ΔR). The entire system was controlled by the personal computer.

^{a)}Electronic mail: wang@mail.phys.nsysu.edu.tw

III. LINE-SHAPE THEORY

The line shape of electromodulation is a response of field-induced change of the reflectivity, which is written as^{2,3}

$$\frac{\Delta R}{R} = \alpha(\epsilon_1, \epsilon_2) \delta\epsilon_1 + \beta(\epsilon_1, \epsilon_2) \delta\epsilon_2, \quad (1)$$

in which α and β are the Seraphin coefficients, and $\delta\epsilon_1$ and $\delta\epsilon_2$ are the modulation induced changes in the real and imaginary parts, respectively, of the complex dielectric function. Near the band edge, E_0 , of GaAs, $\beta \approx 0$ and $\Delta R/R \approx \alpha \delta\epsilon_1$.

In the case of a flatband condition under an electric field F , $\Delta\epsilon$ is defined as

$$\Delta\epsilon(E, F) = \epsilon(E, F) - \epsilon(E, 0), \quad (2)$$

where E is the photon energy.

Near the E_0 transition of GaAs, $\Delta\epsilon$ is given by¹⁸

$$\Delta\epsilon(E, F) = \sum_i \frac{B_i (\hbar \theta_i)^{1/2}}{E^2} G\left(\frac{E_g - E}{\hbar \theta_i}\right), \quad (3)$$

where $i = hh$ or lh , standing for the heavy- and light-hole contributions, respectively, the B_i are parameters which contain the interband optical transition matrix elements, E_g is the energy gap, and $\hbar \theta_i$ is the electro-optic energy as given by

$$\hbar \theta_i = (e^2 \hbar^2 F^2 / 2 \mu_i)^{1/3}, \quad (4)$$

in which μ_{hh} and μ_{lh} are the reduced masses of heavy, light holes and electron in the direction of F , respectively.

In the case of a uniform built-in electric field F_{bi} and a modulation field δF , it was proposed that⁵

$$\begin{aligned} \delta\epsilon^{PR}(E, F_{bi}) &= \epsilon(E, F_{bi}) - \epsilon(E, F_{bi} - \delta F) \\ &= \Delta\epsilon(E, F_{bi}) - \Delta\epsilon(E, F_{bi} - \delta F), \end{aligned} \quad (5)$$

and

$$\begin{aligned} \delta\epsilon^{ER}(E, F_{bi}) &= \epsilon(E, F_{bi} + \delta F/2) - \epsilon(E, F_{bi} - \delta F/2) \\ &= \Delta\epsilon(E, F_{bi} + \delta F/2) - \Delta\epsilon(E, F_{bi} - \delta F/2). \end{aligned} \quad (6)$$

The main difference between ER and PR is that the former is the difference between the dielectric constant of $F_{bi} + \delta F/2$ and $F_{bi} - \delta F/2$, whereas the latter is that of F_{bi} and $F_{bi} - \delta F$. We can simulate PR by ER under the condition that the sample is at a forward bias of $\delta F/2$, that is,

$$\begin{aligned} \delta\epsilon(E, F_{bi}) &= \epsilon(E, F_{bi} + \delta F/2 - \delta F/2) \\ &\quad - \epsilon(E, F_{bi} - \delta F/2 - \delta F/2) \\ &= \Delta\epsilon(E, F_{bi}) - \Delta\epsilon(E, F_{bi} - \delta F). \end{aligned} \quad (7)$$

The electric fields can be obtained by applying the fast Fourier transform to the PR spectra. This approach has the advantage of determining F without the ambiguity of choosing μ . The frequency, f , evaluated from the Fourier transform is related to F by

$$f_i = \frac{2}{3\pi} (2\mu_i)^{1/2} \left(\frac{1}{e\hbar F} \right), \quad (8)$$

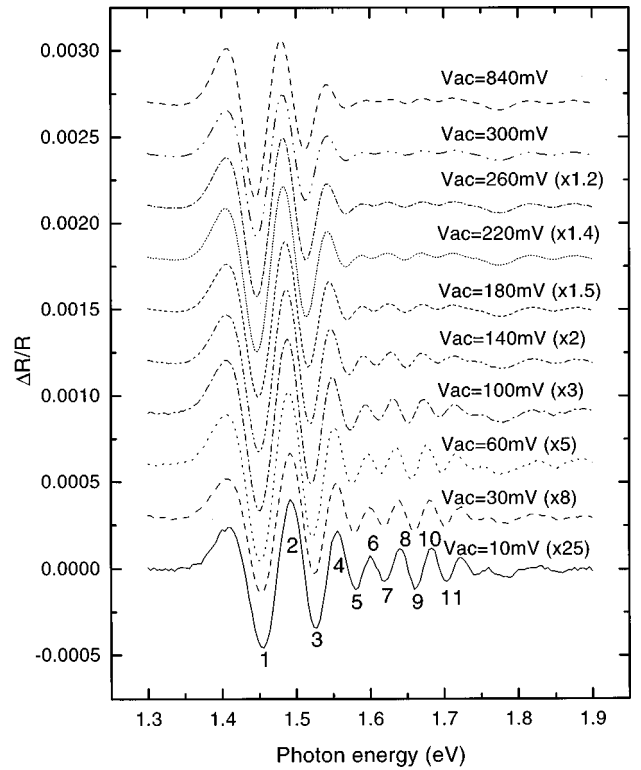


FIG. 1. Electrorreflectance simulated photorefectance at various V_{ac} and the positions of the extrema of FKOs are labeled by the index numbers.

where $i = hh$ or lh , standing for the heavy- and light-hole contributions, respectively.

IV. RESULTS AND DISCUSSIONS

The ER simulated PR spectra and the corresponding FFT of $s-i-n^+$ GaAs for various V_{ac} are shown in Figs. 1 and 2, respectively. The spectra of low values of V_{ac} exhibit many FKOs above the band gap energy. This is due to a uniform field existing in the undoped layer. The positions of the extrema of FKOs are labeled by the index numbers. The beat in the FKOs result from the different oscillation frequencies associated with the transitions of the heavy and light holes, due to different μ values. Their FFT spectra are resolved into two peaks, which corresponds to heavy- and light-hole transitions, respectively.

The advantage of using ER to simulate PR is that the magnitude of δF can be determined more precisely. We have measured ER spectra at various bias (V_{bias}). The F 's thus obtained, which were deduced from the periods of FKOs of ER spectra, are shown in Fig. 3 plotted against V_{bias} . These are close to being linear which show that the field in the undoped layer is nearly uniform. From the relation between F and V_{bias} [$F(\text{V/cm}) = 76919 (\text{V/cm}) - 80877 (1/\text{cm}) \times V_{bias}(\text{V})$], V_{ac} can be transformed to δF in the following way: $\delta F (\text{V/cm}) = 80877 (1/\text{cm}) \times V_{ac} (\text{V})$.

According to Eq. (8), the evaluated F vs δF is shown in Fig. 4. It can be divided into three regions for discussion. Region I is when $\delta F < 16175 \text{ V/cm}$ ($V_{ac} < 200 \text{ mV}$), F decreases with increasing δF . Region II is when $16175 \text{ V/cm} \leq \delta F < 24263 \text{ V/cm}$ ($200 \text{ mV} \leq V_{ac} < 300 \text{ mV}$), F increases

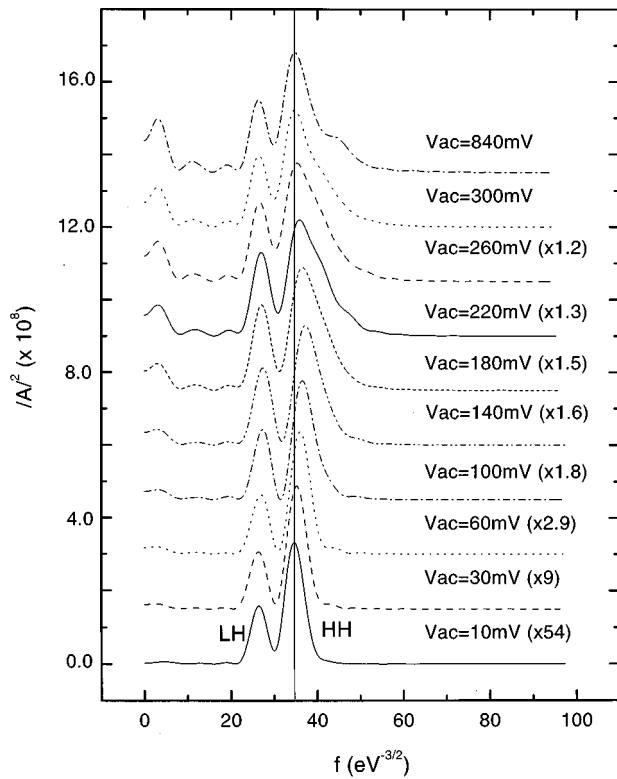


FIG. 2. Fast Fourier transform of Fig. 1, where HH and LH denotes heavy and light hole transitions, respectively.

with increasing δF . Region III is when $\delta F \geq 24263$ V/cm ($V_{ac} \geq 300$ mV), F becomes close to the value of F when δF approaches zero.

According to Eq. (6), $\delta\epsilon^{PR}$ is the difference between $\Delta\epsilon_1(E, F_{bi})$ and $\Delta\epsilon_1(E, F_{bi} - \delta F)$. When δF is increased, the transformed peak will become broader, as shown in Fig. 2. The broadening comes from two reasons. One is when δF increases, the peaks corresponding to $\Delta\epsilon_1(E, F_{bi})$ and $\Delta\epsilon_1(E, F_{bi} - \delta F)$ will be separated more. The other is when δF increases, the amplitude of FKOs will damp out faster with energy so that the effective width for the FFT becomes narrower. Thus the transformed spectrum will become

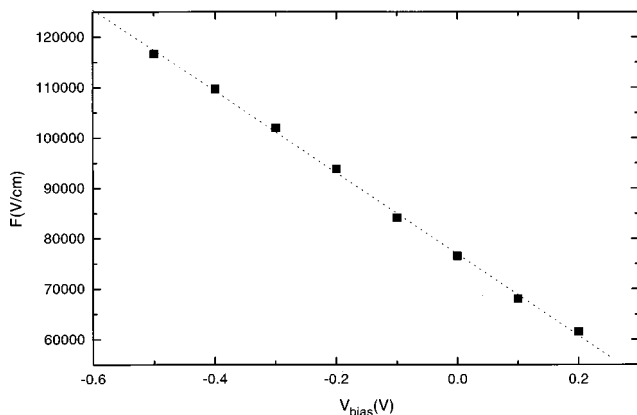


FIG. 3. Strengths of the electric field (F) in the undoped layer are plotted against V_{bias} . The negative value of V_{bias} means reverse voltage. The dashed line is the linear fitting of the data.

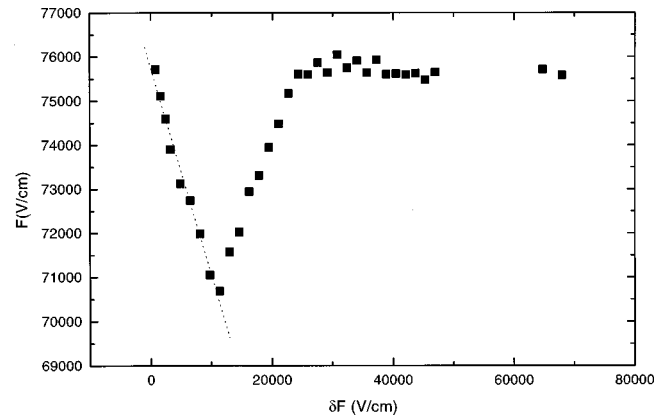


FIG. 4. Strengths of the electric field (F) in the undoped layer are plotted against δF . The straight line represents the equation $F = 75747$ V/cm $- 0.47 \times \delta F$.

broader. This is known from the fact that if the width of the finite wave train is ΔE , then the bandwidth of its FFT spectrum is $4\pi/\Delta E$.

In region I, the data are fitted by a line whose equation is expressed as $F = 75747$ V/cm $- 0.47 \times \delta F$. When $\delta F \ll F_{bi}$, the frequencies of the FKOs are only slightly different. Hence the peaks corresponding to $\Delta\epsilon_1(E, F_{bi})$ and $\Delta\epsilon_1(E, F_{bi} - \delta F)$ will be merged into one peak. The value of the center of the merged peak will be close to the one corresponding to $\Delta\epsilon_1(E, F_{bi} - \delta F/2)$.¹⁵ Hence $F \approx F_{bi} - \delta F/2$ when $\delta F \ll F_{bi}$. Here, we take the value of the intercept as $F_{bi} = 75747$ V/cm.

In region II, where δF becomes larger, it has two effects on the FFT spectra. One is the frequency of $\Delta\epsilon_1(E, F_{bi})$ will become more different from that of $\Delta\epsilon_1(E, F_{bi} - \delta F)$. The other is the amplitude of $\Delta\epsilon_1(E, F_{bi})$ will be greater than that of $\Delta\epsilon_1(E, F_{bi} - \delta F)$. This is because, according to Eqs. (3) and (4), $\Delta\epsilon_1(E, F)$ is proportional to $F^{1/3}$. Hence, when δF is increased, $\Delta\epsilon_1(E, F_{bi})$ will become more dominant. The merged peak will be more unsymmetrical as δF is increased. The value of the peak will be closer to that corresponding to $\Delta\epsilon_1(E, F_{bi})$. Hence, the evaluated F will increase with δF .

In region III, the frequencies of $\Delta\epsilon_1(E, F_{bi})$ and $\Delta\epsilon_1(E, F_{bi} - \delta F)$ are so different that they become separable. Also, the amplitude of $\Delta\epsilon_1(E, F_{bi})$ will become even larger than that of $\Delta\epsilon_1(E, F_{bi} - \delta F)$. Hence, the peak corresponding to $\Delta\epsilon_1(E, F_{bi})$ will be affected little by that of $\Delta\epsilon_1(E, F_{bi} - \delta F)$. Thus the F evaluated from the main peak of FFT is close to that of $\Delta\epsilon_1(E, F_{bi})$.

V. CONCLUSION

Photoreflectance of $s-i-n^+$ GaAs has been simulated by electroreflectance. The FFT can be divided into three regions. Region I is when $\delta F < 16175$ V/cm ($V_{ac} < 200$ mV), F is close to $F_{bi} - \delta F/2$ and the FFT line shape can be clearly resolved into two peaks, which corresponds to heavy- and light-hole transitions, respectively. Region II is when 16175 V/cm $\leq \delta F < 24263$ V/cm (200 mV $\leq V_{ac} < 300$ mV), F increases with increasing δF and the line shape of the heavy-hole transition becomes more unsymmetrical. Region

III is when $\delta F \geq 24263 \text{ V/cm}$ ($V_{ac} \geq 300 \text{ mV}$), F becomes close to F_{bi} and the main peak of the heavy-hole transition becomes the most dominant one.

ACKNOWLEDGMENT

The authors acknowledge the support of the National Science Council of Taiwan, Republic of China, under Contract No. NSC 88-2112-M-110-003.

¹M. Cardona, *Modulation Spectroscopy* (Academic, New York, 1969).

²D. E. Aspnes, in *Handbook on Semiconductors*, edited by T. S. Moss (North-Holland, New York, 1980), Vol. 2, p. 109.

³F. H. Pollak, in *Handbook on Semiconductors*, edited by M. Balkanski (North-Holland, New York, 1994).

⁴H. Shen and M. Dutta, *J. Appl. Phys.* **78**, 2151 (1995).

⁵See, for example, R. N. Bhattacharya, H. Shen, P. Parayanthal, and F. H. Pollak, *Phys. Rev. B* **37**, 4044 (1988).

⁶D. E. Aspnes, *Phys. Rev.* **147**, 554 (1966).

⁷X. Yin, H.-M. Chen, F. H. Pollak, Y. Chan, P. A. Montano, P. D. Kirchner, G. D. Pettit, and J. M. Woodall, *Appl. Phys. Lett.* **58**, 260 (1991).

⁸C. Van Hoof, K. Deneffe, J. DeBoeck, D. J. Arent, and G. Borghs, *Appl. Phys. Lett.* **54**, 608 (1989).

⁹H. Shen, M. Dutta, L. Fotiadis, P. G. Newman, R. P. Moerkirk, W. H. Chang, and R. N. Sacks, *Appl. Phys. Lett.* **57**, 2118 (1990).

¹⁰M. Sydor, J. R. Engholm, M. O. Manasreh, C. E. Stutz, L. Liou, and K. R. Evans, *Appl. Phys. Lett.* **56**, 1769 (1990).

¹¹T. M. Hsu, Y. A. Chen, M. N. Chang, N. H. Lu, and W. C. Lee, *J. Appl. Phys.* **75**, 7489 (1994).

¹²D. P. Wang and C. T. Chen, *Appl. Phys. Lett.* **67**, 2069 (1995).

¹³V. L. Alperovich, A. S. Jaroshevich, H. E. Scheibler, and A. S. Terekhov, *Solid-State Electron.* **37**, 657 (1994).

¹⁴M. Hecht, *Phys. Rev. B* **1**, 7918 (1990).

¹⁵D. P. Wang, C. C. Chen, T. L. Shen, T. M. Hsu, and W. C. Lee, *J. Appl. Phys.* **80**, 6980 (1996).

¹⁶H. Shen, M. Dutta, R. Lux, W. Buchwald, L. F. Fotiadis, and R. N. Sacks, *Appl. Phys. Lett.* **59**, 321 (1991).

¹⁷D. P. Wang, *Appl. Phys. Lett.* **74**, 3 (1999).

¹⁸D. E. Aspnes and A. A. Studna, *Phys. Rev. B* **7**, 4605 (1973).